URSI-RCRS 2024, ARIES/GEHU, Bhimtal, India, 22 - 25 October, 2024

Eclipse in Spider MSP J1908+2105: Probing into the Highly Magnetized Stellar Wind via Polarization and Emission Variations

Ankita Ghosh*(1), Bhaswati Bhattacharyya(1), Sangita Kumari(1), Arpan Pal(1)
(1) National Centre For Radio Astrophysics, Tata Institute of Fundamental Research, Pune 411007, India

Abstract

Eclipses in spider MSPs can reveal the extremely magnetized environments of their companions, shedding light on interactions between pulsar and stellar winds and the highly energetic particles in these harsh conditions. However, comprehensive wideband polarization studies of these systems remain scarce. PSR J1908+2105, with a 3.5-hour orbital period and a companion with mass 0.055 $M_\odot$, bridges the gap between black widow and redback spider population. We present a detailed study of eclipses and polarization in this rare spider MSP using wide-band observations with the uGMRT (300−500 MHz) and Parkes UWL (704−4032 MHz). Our study reveals that it exhibits extended eclipses at unusually high frequencies, making it only the third such system known and the first to have its eclipse mechanism studied. We identify synchrotron absorption as the primary eclipse mechanism. Orbital phase-resolved polarization analysis shows depolarization near the pulsar's superior conjunction, indicating a strong magnetic field in the eclipse region for the first time in this MSP. We also constrained the emission geometry by fitting the rotating vector model (RVM) to the polarization angle sweep. Notably, we report the first evidence of lensing effects near eclipse boundaries for this MSP, leading to significant magnification of the radio emission, a phenomenon observed in only other three spider MSPs. Additionally, we modeled the electron density near the eclipse boundary to explain the observed material trail. This research enhances our understanding of the intense conditions within the eclipsing medium of spider MSPs, providing insights into the dynamics of these extreme binary systems.

1 Introduction

Millisecond pulsars (MSPs) in compact binary orbits having a low-mass non-degenerate or partially non-degenerate companion with an orbital period of less than a day are known as "spider MSPs"(1). Depending on the mass of the companion (M_c), these spider MSPs are further divided into two categories; "black widow (BW)" ($M_c < 0.05\ M_\odot$) and "redback (RB)"($0.1\ M_\odot < M_c < 0.9\ M_\odot$) spiders. As the pulsar and the companion are in very close proximity, in these systems, the highly energetic wind from the pulsar ablates the companion. Material blown from the companion causes an eclipse by obscuring the pulsar's radio emission. Frequency-dependent eclipsing is reported for a majority of known spider MSPs. Understanding the eclipse mechanism allows us to investigate the properties of eclipsing materials as well as the interpretation of the intrabinary shock that happens in these systems as a result of stellar wind and relativistic pulsar wind interaction.

Analyzing the polarization of spider pulsars reveals the presence of a substantial magnetic field within the eclipse medium. This offers a unique opportunity to investigate the eclipse mechanism involving cyclo-synchrotron absorption. According to (2), variations in the RM near the eclipse boundary of PSR J2256−1024 suggest a line-of-sight magnetic field strength of approximately 1.11 mG. (3) analyzed the polarization properties of PSR J2051−0827, deriving tentative constraints on the line-of-sight magnetic field (20 ± 120 G) and the (near-) perpendicular field (<0.3 G).

Motivated by this, we present the eclipse and polarization properties of spider pulsar PSR J1908+2105 using the observations from the Giant Meter Radio Telescope (GMRT) and Parkes 64 m radio telescope. PSR J1908+2105 was discovered by searching for radio pulsations targetted towards the unidentified Fermi-Large Area Telescope (LAT) source with the 327 MHz receiver of the Arecibo (4). It has a spin period of 2.56 ms and a dispersion measure (DM) of 61.9067 pc/cm^{-3}, with a flux density of 0.6 mJy at 327 MHz. This spider pulsar has an orbital period of 3.51 hrs, a minimum companion mass of 0.055 $M_\odot$, and occupies a region in between black widows and redbacks (5), a rare finding with known spider systems. In this paper, we aimed to constrain the eclipse mechanism of the spider MSP J1908+2105 by modeling electron density distributions and determining the magnetic field through polarization studies.

2 Observations

We conducted follow-up observations of PSR J1908+2105 using uGMRT band−3 (300−500 MHz) in coherently dedispersed (CD) mode. Additionally, observations were performed using the Parkes Ultra-Wideband (UWL) receiver (704−4032 MHz) in full Stokes mode covering nearly one complete orbit of the pulsar aimed at polarization studies across the pulsar's orbit.

3 Electron density distribution near eclipse

PSR J1908+2105 shows an eclipse for approximately 40% of its orbit at 400 MHz. We were able to observe the ingress (when the pulsar is entering the eclipse) of the eclipse only during one epoch, while the egress (when the pulsar is coming out of the eclipse) was observed in three epochs using uGMRT

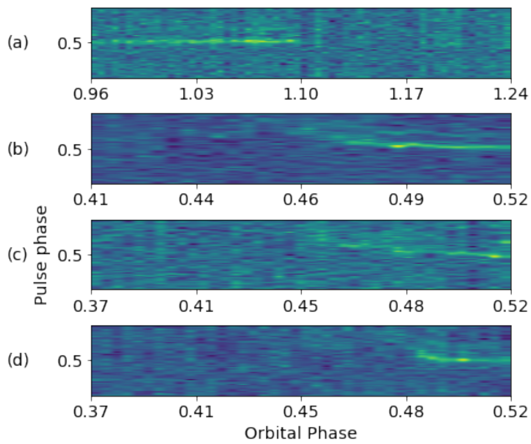

Figure 1. Eclipse boundary variation in different epochs observed with uGMRT at 400 MHz; panel (a): Ingress (when MSP is entering into eclipse); panel (b),(c),(d): Egress (when MSP coming out of the eclipse) as observed with uGMRT at different epochs

band−3 observations. During the ingress of the MSP, there is a sharp decline in flux density (Figure 1), whereas, during eclipse egress, the flux density gradually decreases, leaving a distinct trail of materials (Figure 1). The orbital phase at which the pulse reappears at 400 MHz observed to vary between 0.447 and 0.485, translating to an approximately 8-minute difference. This variability suggests that the boundary of ablated material around the companion is not sharply defined causing an unstable and turbulent egress. Table 1 details temporal shifts of eclipse boundaries corresponding to different epochs. The eclipse boundary is determined by observing the signal-to-noise ratio of sub-integrations near the eclipse region, specifically where the SNR falls below 4. The change of orbital

Table 1. Temporal change of eclipse boundaries

Backend	Frequency (MHz)	Date of observations	eclipse boundary	orbital phase
Parkes UWL	2368	21 Oct 2023	egress	0.34>, <0.45
		31 oct 2023	ingress	0.125 ± 0.002
uGMRT	400	16 Dec 2023	egress	0.475 ± 0.002
		16 Dec 2023	ingress	1.098 ± 0.005
		16 Dec 2023	egress	0.447 ± 0.004
		04 Feb 2024	egress	0.485 ± 0.002

Notes.
The eclipse boundary was determined where the signal-to-noise ratio drops below 4σ.

phase corresponding to an e-folding of local column density is ~ 0.0047 at eclipse ingress. During this time the companion star advances in its orbit by about 25,000 km. At eclipse egress, the e-folding length scale is about 3 times larger ~ 0.0157. During this time the companion star advances in its orbit by about 86,000 km; explaining the long trail observed near egress. At 400 MHz, GMRT observations show ΔDM ~ 0.02 pc cm^{-3} near orbital phase $\phi = 0.48$ during egress. However, moving closer to the companion, at 2368 MHz, Parkes observations show ΔDM ~ 0.6 pc cm^{-3} near $\phi = 0.455$. Similarly, during ingress, uGMRT observations show ΔDM ~ 0.013 pc cm^{-3} near $\phi = 0.09$, increasing to 0.18 pc cm^{-3} at 2368 MHz near $\phi = 0.125$, indicating a sharp rise in DM at egress compared to ingress when we move closer towards the companion. Despite the usual trend of eclipse duration decreasing with frequency, this MSP exhibits a remarkably prolonged eclipse, exceeding 30% of the orbit even at frequencies above 3 GHz. Such eclipses at high frequencies are exceedingly rare and, to our knowledge, have been reported for only two other spider MSPs (e.g. PSR J1723−2837 and J1731−1847). This necessitates constraining the eclipse mechanism specific to this case, which can account for eclipses occurring even at such high frequencies. While the system's short orbital period and relatively small companion mass align with characteristics typical of black widow pulsars, the extended eclipses are typical characteristics of redback pulsars. This suggests the presence of an unusual companion size or a dense plasma distribution surrounding the companion, as discussed in (5). This MSP system may represent a distinct subgroup among spider MSPs, exhibiting features that bridge the characteristics of known black widow and redback pulsars.

4 Orbital Phase-resolved flux density, DM and polarization variations

The total intensity vs. orbital phase is shown in Figure 2 for observations at 400 MHz, and the first panel of Figure 4 shows the flux density variation at 2368 MHz. Similar to PSR J2051−0827, we observed enhanced flux density and increased brightness in pulsed radiation near the first eclipse boundary (Figure 2), which we interpreted as lensing due to circumstellar plasma around the companion near the superior conjunction of the pulsar. In regions with strongly varying electron density, radio emission can be significantly magnified due to plasma lensing. Such extreme plasma lensing has been observed in the black widow pulsar B1957+20 and the redback system B1744−24A, manifesting through highly magnified pulses amplified by factors of 10 over tens of ms. We also detected a few single pulses from the lensed region in the eclipse boundaries. Lensing resolves the pulse emission, constraining emission sizes and component separations, and can be used to infer the velocity of the eclipsing outflow.

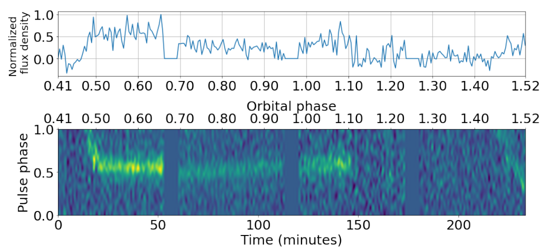

Figure 2. Enhanced flux density and increase in brightness in pulsed radiation near eclipse boundaries observed with uGMRT at 400 MHz on 16 Dec 2023.

In our polarization study of PSR J1908+2105 using Parkes UWL observations (708−4032 MHz), we determined the bestfit rotation measure (RM) value to be 201.30 ± 1.09 rad/m^2 from the integrated average profile (Figure 3). The average pulse profile exhibits approximately 32% linear polarization during the non-eclipse phase, with a relatively low circular polarization fraction of around 2.8%. Our study utilized the full bandwidth of 3328 MHz within the observed frequency range. The polarization position angle (PPA) of PSR J1908+2105 shows an "S" shape swing. Applying the Rotating Vector Model (RVM, (6)) to interpret these swings helped constrain the degeneracy between the angles α (magnetic axis to rotation axis) and β (line of sight to magnetic axis). The resulting distribution resembles a banana shape in chi-square space with $\alpha \sim 92^{\circ}{}^{+40^{\circ}}_{-41^{\circ}}$ and $\beta \sim 32^{\circ}{}^{+5^{\circ}}_{-11^{\circ}}$.

We analyzed intensity, polarization, RM, and DM variations as a function of the orbital phase. We observed a decrease in total intensity and linear polarization fraction and an increase in DM and RM around superior conjunction (orbital phase, 0.12−0.40, Figure 4). Where the average RM is ~ 201 rad/m^2 for the non-eclipse phase, near the eclipse medium RM increases to 230 rad/m^2. The increase in DM and RM shows the increased electron density near the eclipse medium.

Depolarization during the eclipse phase has been observed in spider MSPs; for example, PSR J2051−0827 by (7), PSR J2256−1024 by (2), and J1748−2446A by (8). This depolarization can occur due to the increased RM near eclipse and multipath propagation of pulsed radiation through the circumstellar magnetized plasma leading to rapid time variations in the RM. Such rapid RM variations can result from fluctuations in either or both of the circumstellar components of dispersion measure (DM) and the parallel component of the magnetic field. The maximum DM variations are found to be of the order ~ 0.07 pc cm^{-3} and 0.6 pc cm^{-3} near the ingress and egress boundary respectively, which can not significantly affect the RM. Therefore, short-timescale variations in the line-of-sight magnetic field potentially arising from turbulent stellar wind, can cause depolarization through rapid fluctuations of RM in time, indicating a significant magnetic field in the eclipse medium. During the ingress of the eclipse, the maximum RM is about 230 rad m^{-2} with a ΔRMmax of 30 rad m^{-2} compared to that of the non-eclipse phase. The ΔDM at the orbital phase of ΔRMmax is 0.05 pc cm^{-3}. The line-of-sight magnetic field strength in the eclipse boundary can be estimated by measuring the changes in the Faraday rotation: $B_{||}$=1.23μG$\frac{\Delta RM}{\Delta DM}$=0.9 mG.

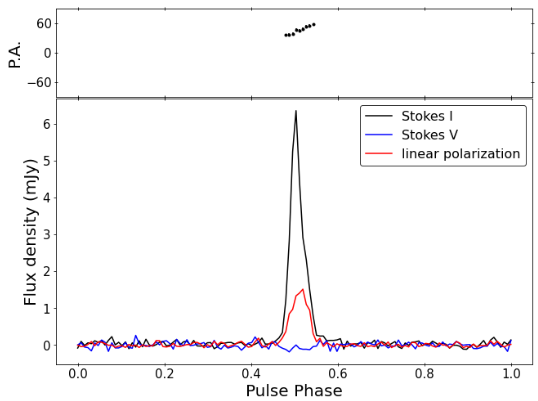

Figure 3. Polarization profile at 2368 MHz from Parkes UWL observations for the non-eclipse region, presenting the first polarization study for J1908+2105.

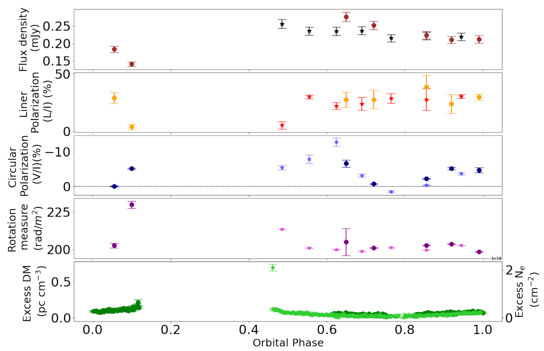

Figure 4. Variation of total intensity, polarization fractions along with RM and DM as a function of orbital phase for PSR J1908+2105 at 2368 MHz from the Parkes UWL observations. Here, the different symbol in a single panel shows observations from different epochs

Similarly, during the egress of the eclipse, the maximum RM is about 213 rad m^{-2} with a ΔRMmax of 13 rad m^{-2} compared to that of the non-eclipse phase. The ΔDM at the orbital phase of ΔRMmax is 0.017 pc cm^{-3}. The line-of-sight magnetic field strength in the eclipse egress is therefore estimated to be ~ 1 mG. For the eclipse medium, we calculated the characteristic magnetic field (B_E), using the pressure balance between pulsar wind energy density ($U_E = \frac{\dot{E}}{4\pi c a^2}$) and the stellar wind energy density of the companion ($\frac{B_E}{8\pi}$), where a is the distance between the pulsar and the companion (a $\sim 1.30\ R_{\odot}$) and c is the speed of light. This gives the characteristic magnetic field for PSR J1908 to be ~ 16 G.

5 Eclipse mechanisms

We reviewed various possible eclipse mechanisms for this system, including refraction, dispersion delay-induced pulse broadening, free-free absorption, cyclotron and synchrotron absorption. Figure 5 shows total intensity and excess DM near eclipse ingress and egress at 400 MHz. The companion's Roche lobe radius R_L is estimated $\sim 0.21 R_{\odot}$. However, the obscured portion of the companion's orbit extends to extends to 1.48 $R_{\odot}$, quite larger than the Roche lobe, indicating it's not gravitationally bound to the companion. PSR J1908+2105 shows a complete eclipse from 400−4000 MHz, allowing electron density assessment near the eclipse boundary only. At egress, the pulse arrival time delay at 400 MHz is $\sim 484\ \mu$s, corresponding to a DM rise of 0.022 pc cm^{-3} and an electron density increase of 8×10^{16} cm^{-2}.

If the pulsar's radio frequency is lower than the plasma frequency of the eclipsing medium, it obscures the signal. Given the electron density N_e at the eclipse boundaries, the plasma cutoff frequency $f_p \sim 5.37$ MHz, is much lower than the observed frequencies. Achieving an eclipse due to plasma cutoff is impossible as it requires an extremely high electron density.

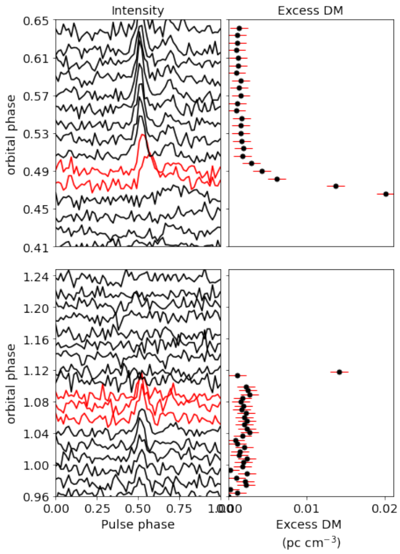

Figure 5. Total intensity, I (black) for average pulse profiles of PSR J1908+2105 during the ingress (bottom panels) and egress (upper panels) of the eclipse from uGMRT observations at 400 MHz. The red lines are the last and first pulses before and after the eclipse. The pulse profiles near the eclipse become wider. The corresponding DM (black dots) variations of the eclipse are shown in the right panels. The red bars are the errors on the DM.

Refraction-induced eclipse is also unlikely due to the required pulse delay being much greater than the observed delays. Additionally, pulse smearing and scattering don't account for the eclipses, as the observed delays and scattering timescales ($\tau \sim$ 0.06 ms at 400 MHz and 0.09 ms at 2368 MHz) are less than one-fifth of the pulse period. For induced Compton scattering, the optical depth is less than one at both 400 and 2368 MHz, making it an unfeasible eclipse mechanism. Free-free absorption could occur if plasma temperatures were extremely low or clumping factors very high, but these conditions are not physically achievable in the eclipse environment. Cyclotron absorption is not the main mechanism as its required specific temperature conditions are unmet at both low and high frequencies. Therefore we conclude, that synchrotron absorption by trans relativistic non-thermal electrons is the primary mechanism causing eclipse at such extremely high frequency.

6 Summary

PSR J1908+2105 straddles the line between "black widows" and "redbacks." Its short orbital period, low companion mass, and extensive eclipses make it an atypical "spider" variant. Key findings from our first polarimetry and detailed eclipse study include: 1. Electron density modeling around the companion explaining material trails at eclipse boundaries. 2. Linear depolarization and increased RM near the eclipse suggest high electron density and magnetic fields up to 16 G near the companion. 3. Eclipses above 3 GHz have been seen in the other two spider MSPs, but detailed studies are lacking. For PSR J1908+2105, synchrotron absorption is the primary eclipse mechanism. 4. Emission geometry is constrained from the observed position angle (PPA) swing and has been done for very few spider MSPs. 5. Lensing effects near eclipse boundaries, observed at uGMRT band−3, highlight opportunities for detailed emission geometry analysis and comprehensive modeling of the eclipse medium.

References

[1] M. S. E. Roberts, "Surrounded by spiders! New black widows and redbacks in the Galactic field," in *Neutron Stars and Pulsars: Challenges and Opportunities after 80 years*, J. van Leeuwen, Ed., vol. 291, March 2013. doi: 10.1017/S174392131202337X pp. 127–132.

[2] K. Crowter, I. H. Stairs, C. A. McPhee, A. M. Archibald, J. Boyles, J. Hessels, C. Karako-Argaman, D. R. Lorimer, R. S. Lynch, M. A. McLaughlin, S. M. Ransom, M. S. E. Roberts, K. Stovall, and J. van Leeuwen, "The GBT 350-MHz Drift Scan Pulsar Survey - III. Detection of a magnetic field in the eclipsing material of PSR J2256-1024," , vol. 495, no. 3, pp. 3052–3064, July 2020. doi: 10.1093/mnras/staa933

[3] E. J. Polzin, R. P. Breton, B. W. Stappers, B. Bhattacharyya, G. H. Janssen, S. Osłowski, M. S. E. Roberts, and C. Sobey, "Long-term variability of a black widow's eclipses - A decade of PSR J2051-0827," , vol. 490, no. 1, pp. 889–908, November 2019. doi: 10.1093/mnras/stz2579

[4] H. T. Cromartie, F. Camilo, M. Kerr, J. S. Deneva, S. M. Ransom, P. S. Ray, E. C. Ferrara, P. F. Michelson, and K. S. Wood, "Six New Millisecond Pulsars from Arecibo Searches of Fermi Gamma-Ray Sources," , vol. 819, no. 1, p. 34, March 2016. doi: 10.3847/0004-637X/819/1/34

[5] J. S. Deneva, P. S. Ray, F. Camilo, P. C. C. Freire, H. T. Cromartie, S. M. Ransom, E. Ferrara, M. Kerr, T. H. Burnett, and P. M. S. Parkinson, "Timing of Eight Binary Millisecond Pulsars Found with Arecibo in Fermi-LAT Unidentified Sources," , vol. 909, no. 1, p. 6, March 2021. doi: 10.3847/1538-4357/abd7a1

[6] V. Radhakrishnan and D. J. Cooke, "Magnetic Poles and the Polarization Structure of Pulsar Radiation," , vol. 3, p. 225, January 1969.

[7] S. Q. Wang, J. B. Wang, D. Z. Li, J. M. Yao, R. N. Manchester, G. Hobbs, N. Wang, S. Dai, H. Xu, R. Luo, Y. Feng, W. Y. Wang, D. Li, Y. W. Yu, Z. X. Du, C. H. Niu, S. B. Zhang, and C. M. Zhang, "Change of Rotation Measure during the Eclipse of a Black Widow PSR J2051-0827," , vol. 955, no. 1, p. 36, September 2023. doi: 10.3847/1538-4357/acea81

[8] X. P. You, R. N. Manchester, W. A. Coles, G. B. Hobbs, and R. Shannon, "Polarimetry of the Eclipsing Pulsar PSR J1748-2446A," , vol. 867, no. 1, p. 22, November 2018. doi: 10.3847/1538-4357/aadee0